GMR
The Original

FORMULATION AND EVALUATION OF NARINGENIN-LOADED SPANLASTICS TOPICAL GEL FOR THE TREATMENT OF ACNE VULGARIS

[1*]Revati Dharampal Sagare, [1]Kallis D' Souza, [1]Fatima S Dasankoppa, [1]Pratiksha S Akki, [2]Hasanpasha N Sholapur, [3]Rajat Sagare

[1]Department of Pharmaceutics, KLE College of Pharmacy, Hubballi, Karnataka, India-580031. (A Constituent Unit of KLE Academy of Higher Education and Research, Belagavi, Karnataka, India).
[2]Department of Pharmacognosy, KLE College of Pharmacy, Hubballi, Karnataka, India-580031. (A Constituent unit of KLE Academy of Higher Education and Research, Belagavi, Karnataka, India).
[3]Department of Livestock Farm Complex-VMD, Veterinary College Koila, Kadaba, Dakshin Kannada, Karnataka, India – 574241.
*Corresponding Author: Revati Dharampal Sagare, Email id: rdsagare@kledeemeduniversity.edu.in

ABSTRACT

Background: Acne vulgaris is a prevalent chronic inflammatory dermatological disorder, marked by the impedance of hair follicles and sebaceous glands.

Aim: The current research aimed to develop, optimize and characterize a Naringenin-loaded spanlastic topical gel formulation for the effective treatment of acne vulgaris.

Materials and Methods: Spanlastics, an elastic nanovesicles composed of Span 60 and Tween 80, were formulated using the ethanol injection method. The formulated spanlastics were optimized by 2^3 Factorial design using Design of Experiments Software. The selected independent variables include: concentration of Span 60 (X_1), Tween 80 (X_2) and Sonication time (X_3). The dependent variables includes: Particle size (Y_1), % Encapsulation efficiency (Y_2) and Zeta potential (Y_3). The optimized spanlastics formulation was incorporated into a gel base. The prepared gel was evaluated for various characterization studies such as pH, viscosity and drug content. Morphological characterization was performed using transmission electron microscopy (TEM). In vitro drug release studies were performed to assess the release kinetics. Stability studies were carried out in accordance to ICH guidelines at accelerated storage conditions for three months.

Results and Discussion: The optimized spanlastics formulation showed a particle size of 157.7 nm, with a zeta potential of -32.4 mV and an entrapment efficacy of 89.4 %. The TEM analysis confirmed the presence of uniformly distributed spherical vesicles. The gel formulations exhibited pH values in the range of 6.9 to 7.3, with a viscosity ranging from 2884 to 5987 cps and drug content of 78 – 85 %. The in vitro release was within the range of 72.49 to 95.36 %. The results of minimum inhibitory concentration of naringenin against *P. acnes* was 0.8 µg/ml, indicating its potential as an effective antibacterial agent at this concentration.

Conclusion: In conclusion, naringenin-loaded spanlastics gel demonstrated an improved skin permeation, sustained release and notable antimicrobial activity, suggesting its potential as an effective topical treatment for acne vulgaris.

KEYWORDS: Acne vulgaris, Naringenin, Spanlastics, Topical gel, Nano-carriers, Optimization.

INTRODUCTION

Acne Vulgaris commonly termed as "Acne" is a chronic pilosebaceous inflammatory skin disorder, affecting approximately > 85 % of adolescents and persisting into adulthood worldwide. In accordance to the epidemiological estimates derived from Global Burden of Disease Study 2021, Acne is projected to affect approximately 9-10 % of global population, representing one of the most widespread disease worldwide across different age groups. Acne predominantly affects the majority of adolescents and often persists into adulthood, especially in females, contributing to nearly two-thirds of acne related dermatological consultations [1]. Acne vulgaris poses a considerable impact on the standard of living of teenagers, particularly in male populations as compared to females, due to higher androgen levels, which promote greater sebum production. Acne can either persist from adolescence as persistent acne or arise de novo in adulthood as late-onset acne. The enduring nature and extensive prevalence of both persistent acne and late-onset acne impose a significant public health concern across all age demographics. Although acne is a non-fatal condition, it significantly contributes to morbidity and negatively impacts the quality of life, emphasizing the necessity for an effective therapeutic approaches [2].

The management of acne vulgaris constitutes a wide variety of therapeutic strategies, including topical agents such as benzoyl peroxides, retinoids, salicylic acid and topical antibiotics such as clindamycin and erythromycin. In consistence to this, the treatment approaches for acne constitutes the systemic therapies such as oral antibiotics and various hormonal agents. Although, these conventional therapies offer certain level of effectiveness, but their long term use is often associated with adverse effects, skin irritation and inadequate patient compliance. Thus, these limitations have sparked an increasing interest in innovative nano-structured vesicular drug delivery strategies that aims to enhance the therapeutic efficacy while minimizing the side effects [3].

Vesicular drug delivery systems are novel and versatile carrier systems designed to enhance the therapeutic efficacy and safety of drug molecules by encapsulation within micro-to nano sized vesicles, typically in the range of 50 – 500 nm.

Vesicular systems are defined as well organized closed, spherical structures composed of one or more concentric bilayers formed by the virtue of cluster of amphiphilic molecules in presence of water. Vesicular systems such as transferosome, ethosome, liposome, cubosome, noisome and spanlastics can incorporate both hydrophilic and lipophilic drugs [4]. Spanlastics (SPs) represents a novel therapeutic nano-vesicular carrier based on non-ionic surfactants. SPs are elastic and deformable nanoscale vesicles composed of edge activators (Tween) and non-ionic surfactants (Span), contributing to the nano-scale structure and high elasticity. These nano-vesicular carriers effectively transport a variety of drug molecules within a bilayer structure surrounded by a core cavity. Spanlastics are spheroidal structures comprising of amphiphilic molecules, acting as an appropriate matrices for encapsulation of biological materials. SPs are designed and developed to enhance drug permeation and bioavailability. The elastic and high deformability structure of SPs facilitates for an effective penetration through biological barriers, making them more appropriate for topical and transdermal drug delivery system [5].

Spanlastics represent a promising approach for addressing significant challenges in topical drug delivery, including poor solubility, limited permeability, and reduced skin retention. Their elastic characteristics, coupled with the ability to enhance drug stability and bioavailability, make them a valuable platform for the development of advanced pharmaceutical and dermatological formulations. Their biocompatibility and capacity to penetrate skin barriers render them effective for a broad range of topical and transdermal applications, including anti-inflammatory, antioxidant, and anticancer treatments [6]. The improved retention of Spanlastics within the skin ensures prolonged localization of the drug at the target site, thereby enhancing therapeutic efficacy and reducing systemic side effects. Spanlastics significantly enhance the topical bioavailability of poorly water-soluble drugs such as naringenin through several mechanisms rooted in their unique structure and composition [7].

Naringenin a naturally occurring flavonoid predominantly present in citrus fruits, has been identified as an incredibly viable bioactive compound in the management of acne vulgaris due to its diverse pharmacological properties. Recent studies have identified naringenin as a potential therapeutic compound due to its ability to combat inflammation, improve insulin sensitivity, manage obesity, and support intestinal health. These findings suggest that naringenin may be a valuable natural agent in the treatment of various metabolic and inflammatory conditions [8]. In addition to this, naringenin exhibits significant anti-bacterial activity against Cutibacterium acnes, the primary microorganism involved in acne pathogenesis, thereby reducing microbial colonization within the pilosebaceous unit. Similarly, naringenin possesses potent anti-inflammatory effects by regulating key inflammatory mediators such as tumor necrosis factor-alpha (TNF-α) and interleukins, and by inhibiting the signaling pathways like NF-κB, which are responsible for the development of erythema and swelling in acne lesions. Naringenin also plays a significant role in controlling sebum production by modulating the lipid synthesis in sebaceous glands, therefore reducing excessive oiliness that leads to follicular occlusion. Furthermore, its potent anti-oxidant activity contributes in scavenging reactive oxygen species and thereby protecting the skin cells from oxidative damage and further inhibiting the development of inflammatory lessions. However, the clinical application of naringenin is often limited due to poor aqueous solubility and bioavailability necessitating the use of advanced vesicular drug delivery systems such as liposomes, noisomes and spanlastics [9].

Hence, the present study aims to develop and evaluate naringenin-loaded spanlastics gel formulations as a novel topical delivery system for the effective management of acne vulgaris.

MATERIALS AND METHODS

Materials

Naringenin was purchased from Sisco Research Laboratories, Mumbai, India. Span 60 was purchased from Loba Chemie Pvt Ltd, Mumbai, India. Tween 80 was purchased from S D Fine Chemicals Pvt Ltd, Mumbai, India. Hydroxy Propyl Methyl Cellulose and Xanthum Gum was purchased from S D Fine Chemicals Pvt Ltd, Mumbai, India.

METHODOLOGY

Determination of λ max of Naringenin using UV Spectrophotometer

An accurately weighed quantity of Naringenin (10 mg) was dissolved in a clean, dry volumetric flask (10 ml) and the volume was made up to the mark with the phosphate buffer (7.4 pH) to obtain a standard stock solution of 1000 µg/ml (1 mg/ml – SS-I). From the above stock solution, subsequent dilutions were prepared using 7.4 pH Phosphate buffer. The solutions were analyzed using double beam UV Spectrophotometer (Shimadzu – 1900 i) in the wavelength ranging from 200 – 400 nm [10].

Determination of Standard Calibration Curve of Naringenin

The standard calibration curve of naringenin was determined using UV Visible Spectrophotometer. Accurately weighed quantity of naringenin (10 mg) was transferred to a volumetric flask containing 100 ml of 7.4 pH phosphate buffer to obtain the concentration of primary stock solution of 100 µg/ml. From the above stock solution, an appropriate aliquots were withdrawn and further diluted with 7.4 pH phosphate buffer to obtain a series of standard solutions in the concentration range of 2 – 100 µg/ml. The absorbance of each prepared standard solution was measured at the selected λ max against blank solution. The calibration curve was constructed by plotting concentrations on the x-axis and absorbance values on the y-axis, followed by determination of the linear regression equation [10].

Determination of Drug – Polymer Compatibility Study

By Fourier Transform Infrared Spectroscopy (FTIR Study)

The FT-IR spectrum technique was employed to investigate the physical and chemical interactions between the drug and the excipients used. A mixture containing the Active Pharmaceutical Ingredient (Naringenin) and excipients in the ratio of 1:1 was stored in an amber-colored bottle, placed in a stability chamber at the temperature of 30ºC ± 2ºC with a relative

humidity (RH) of 65 ± 5 % for one month. The samples were analyzed using FTIR spectrophotometer (IR Spirit, Shimadzu, Japan). The samples were scanned and measured and measured in the range of 4000 – 400 cm-1 and the FTIR spectra were recorded and interpreted [11].

Formulation of Naringenin-Loaded Spanlastic Nanoparticles

Naringenin-loaded spanlastics were prepared using the ethanol injection technique. Naringenin and Span 60 were dissolved in 10 mL of ethanol to form the organic phase. This solution was then gradually injected into 50 mL of a preheated aqueous phase containing Tween 80, maintaining a 1:5 ratio of organic to aqueous phases. Various formulations were developed by altering the ratio of Span 60 to Tween 80. The vesicles formed spontaneously, resulting in slight turbidity of the hydroalcoholic solution. The dispersions were continuously stirred to ensure complete evaporation of ethanol. To enhance vesicle formation and reduce particle size, the dispersions were further processed by sonication using a high-intensity ultra-probe sonicator [12].

Experimental Design

An experimental study were designed with two-level three factorial design (2^3) for statistical optimization of naringenin-loaded spanlastics. Design-Expert Software® (Version 13.2. Stat-Ease, Inc., Minneapolis, MN, USA) was employed to generate and evaluate the mathematical relationships between input and output variables in an experimental design. In this experimental design, concentration of Span 60 (X_1), concentration of Tween 80 (X_2) and sonication time (X_3) were selected as an independent variables with two varied levels (low and high). The particle size (Y_1), Zeta potential (Y_2) and % entrapment efficacy (Y_3) were set as dependent variables [13]. The selected independent and dependent variables along with their coded and actual values are demonstrated in Table 1.

Table 1: Two-level three factorial design for optimization of naringenin-loaded spanlastics

Factors (Independent Variables)	Levels	
	Low (-1)	High (+1)
X_1: Concentration of Span 60 (mg)	100	180
X_2: Concentration of Tween 80 (mg)	30	90
X_3: Sonication Time (min)	4.5	9
Dependent Variables	**Desirability Constraints**	
Y_1: Particle Size	In-range	
Y_2: Zeta Potential	In-range	
Y_3: Entrapment Efficacy (%)	In-range	

Table 2: Composition of two-level three factorial experimental design for optimization of Naringenin - loaded spanlastics

Run	Factor levels in actual values		
	X_1: Concentration of Span 60 (mg)	X_2: Concentration of Tween 80 (mg)	X_3:Sonication Time (min)
1	180	90	4.5
2	180	90	9
3	180	30	9
4	100	90	4.5
5	100	90	9
6	180	30	4.5
7	100	30	4.5
8	100	30	9

Characterization of Naringenin-loaded spanlastics

Particle size and Zeta Potential

The average particle size and zeta potential of the prepared naringenin-loaded spanlastics were determined by using dynamic light scattering technique (DLS), while zeta potential was determined using Nano ZS ZS90 instrument (Malvern Instruments, UK). The procedure was carried out with 1 ml of spanlastic formulation diluted with 10 mL of Milli-Q water. All measurements were performed at 25°C using folded capillary cells (DTS 1060), with each test performed in triplicate to ensure accuracy and reproducibility [14].

Entrapment Efficiency (%)

The Naringenin-loaded spanlastic dispersions were centrifugation at 19,000 rpm for 10 minutes using a high-speed refrigerated centrifuge (Floor Model, 7000 Kubota, Japan). The supernatant was then carefully collected, appropriately diluted, and analyzed for Naringenin content using UV/Visible spectrophotometry at 290 nm [14].

The % EE was calculated

$$\% EE = \frac{Total\ drug\ entrapped - Amount\ of\ drug\ in\ supernatant}{Total\ drug\ entrapped}\ x\ 100 \quad \text{---------- (1)}$$

Morphological Study

Transmission Electron Microscopy

The morphology of spanlastics was assessed using a field emission gun transmission electron microscope (JEOL® JEM-2100F, Japan) operated at an accelerating voltage of 120/200 kV. A drop of the spanlastic dispersion was applied onto a carbon-coated copper grid and stained with 1% phosphotungstic acid for 2–3 minutes. After air drying, the sample was examined under the microscope [15].

Content Analysis

The content analysis of spanlastic formulation was analyzed using the dynamic dialysis method. The formulation was dialyzed against phosphate-buffered saline (pH 7.4) for 15–20 minutes using a dialysis membrane with a molecular weight cut-off of 12,000–14,000 Da to remove unencapsulated drug. Dialysis was repeated until no drug was detected in the dialysate. To lyse the spanlastic vesicles, 1 mL of the dialyzed sample was combined with ethanol and sonicated for 15 minutes, resulting in a clear solution. A 0.1 mL aliquot of this solution was then diluted with PBS (pH 7.4), filtered, and analyzed for drug content by UV spectrophotometry at 290 nm using a calibration curve [15].

Preparation Naringenin-loaded Spanlastic Gel

The selected optimized formulation from experimental design was incorporated into topical gel using Hydroxy Propyl Methyl Cellulose (HPMC) and xanthan gum as gelling agent. The required amount of HPMC and xanthan gum was dissolved in 10-15 ml of purified water with continuous stirring and allowed to hydrate overnight. Subsequently, naringenin-loaded spanlastic dispersion was incorporated with gentle stirring to ensure uniformity and minimize air entrapment. The pH was adjusted to 6.0 – 7.0 by adding triethanolmanie drop-wise, with gentle stirring after each addition. Purified water was added to make up the total weight to 30g. The gel was mixed thoroughly and transferred into a clean, light-resistant container, and stored at room temperature [16]. The formulation of naringenin-loaded spanlastics gel is presented in Table no 3.

Table no 3: Formulation of Naringenin-loaded Spanlastics Topical Gel

Ingredients	GG1	GG2	GG3	GG4
Naringenin loaded Spanlastics dispersion (ml)	50	50	50	50
Hydroxy Propyl Methyl Cellulose (%)	1	1.5	-	-
Xanthan Gum (%)	-	-	1	1.5
Tri ethanol amine (%)	0.2	0.2	0.2	0.2
Distilled water	q.s	q.s	q.s	q.s

Characterization of Naringenin-loaded Spanlastic topical Gel

Determination of pH

The pH of the formulated gels were determined at room temperature using a digital pH meter, which was calibrated with buffer solutions of pH 4.0, 7.0 and 10.0 prior to the measurement.

Determination of Viscosity of Gel

The viscosity of the prepared gel formulations was assessed using an Anton Paar Brookfield DV-2T viscometer, operated at a controlled temperature of 25 ± 0.5°C. Spindle number TL7 was employed at a rotational speed of 50 rpm. Each sample was tested in triplicate to ensure consistency, and the average viscosity was expressed in centipoise (cP).

Determination of Spreadability of Gel

Approximately 1g of Naringenin-loaded spanlastic gel was placed between two glass slides and compressed uniformly. The setup was allowed to stand for 5 min or until no further spreading was observed. The diameter of the circular film formed was then measured and recorded [17].

In-vitro diffusion studies

The in-vitro diffusion studies were carried out using a Franz diffusion cell apparatus. A dialysis membrane, previously soaked overnight in PBS pH 7.4, as a receptor medium. Approximately 1g of the formulated gel was placed on dialysis

membrane between the donar and receptor compartments. The entire assembly was maintained on a magnetic stirrer with controlled temperature settings. The receptor medium was continuously stirred at 50 RPM at the temperature of 37 ± 0.5ºC. At pre-determined time intervals (0.5, 1, 2… 8h), 1ml of sample was withdrawn from the receptor compartment and replaced with an equal volume of fresh receptor medium to maintain sink conditions. The collected samples were analyzed using a UV spectrophotometer at a λmax of 290 nm. The cumulative amount of drug released through the membrane after 8h was calculated.

Stability studies

Short term stability studies of optimized spanlastics nano-formulations and gel was carried out in a stability chamber (Thermolab Scientific Equipments, India) at 40 ± 2ºC and 75 ± 5% RH. Samples were withdrawn at the intervals of 1 and 2 months and evaluated for mean particle size, zeta potential, % EE, viscosity and drug content [18].

Anti-microbial activity of Naringenin

Minimum Inhibitory Concentration

For determination of the minimum inhibitory concentration (MIC), nine serial dilutions of each drug were prepared using thioglycollate broth. Initially, 20 µL of the drug was added to 380 µL of thioglycollate broth in the first tube. Subsequently, 200 µL was transferred to the first dilution tube containing 200 µL thioglycollate broth to obtain a 10^{-1} dilution. This serial dilution procedure was continued sequentially upto 10-9 dilution. A bacterial inoculum was prepared by adding 5 µL of stock culture of 2ml of thioglycollate broth. Thereafter, 200 µL of the prepared inoculum was added to each serially diluted tube. The tubes were then incubated in an anaerobic jar at 37 ºC for 48-72 h and bacterial growth was assessed based on the appearance of turbidity [19].

Statistical Analysis

Naringenin-loaded spanlastics were optimized using Design-Expert ® software. The significance of the developed model and its individual terms were evaluated by analysis of variance (ANOVA).

RESULTS

Pre-formulation

Determination of wavelength of maximum absorption (λmax)

A solution containing Naringenin at a concentration of 10 µg/ml was prepared by dissolving it in a buffer solution with a pH of 6.8. UV spectrum analysis was performed using a Shimadzu (UV-1900i) double beam spectrophotometer, scanning the solution within the wavelength range of 200 – 400 nm. The absorption maximum was found to be 290 nm using 6.8 pH buffer solution as shown in Figure 1.

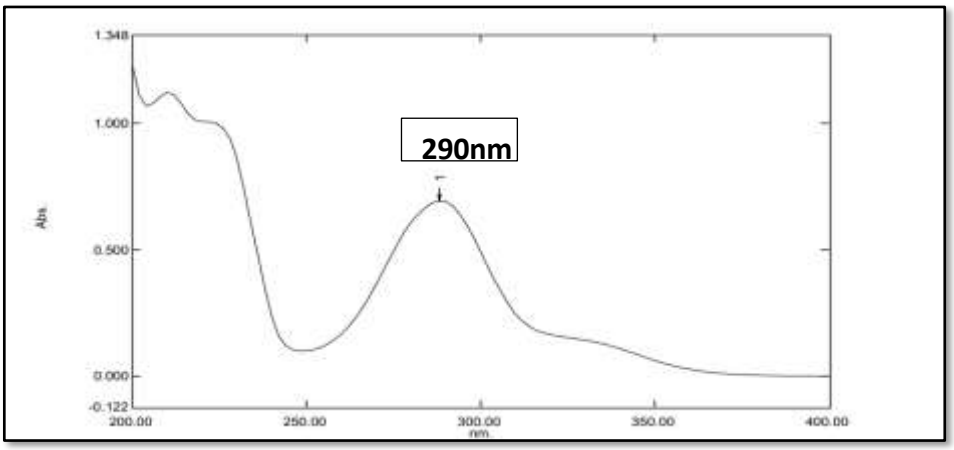

Figure 1: UV Spectrum of Naringenin

Preparation of Standard Calibration Curve of Naringenin

The standard calibration curve of Naringenin was carried out in 7.4 pH phosphate buffer and diluted to obtain the concentration of 10-100 µg/ml. The absorbance values for these solutions were determined at 290 nm using double beam UV Spectrophotometer. The calibration curve obtained for naringenin showed good linearity with a regression co-efficient (R^2) value of 0.99 over the concentration range of 10-100 µg/ml. A graph of concentration in µg/mL v/s absorbance in nm was plotted as shown in Figure 2.

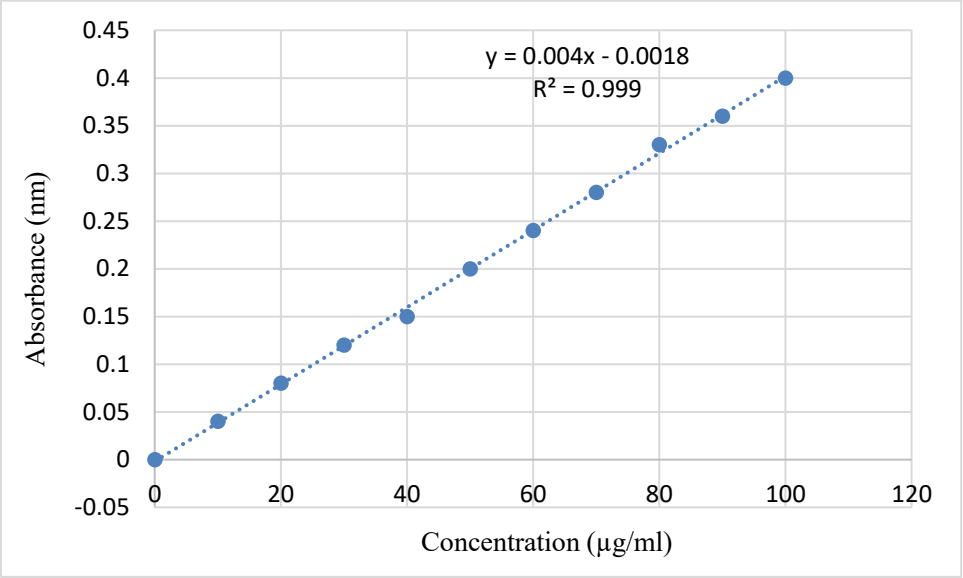

Figure 2: Standard Calibration Curve of Naringenin

FTIR Analysis

The data obtained from FT-IR studies presented in Table 4, indicates that drug and excipients present in the formulation are compatible with each other with no signs of interactions. The FT-IR spectra of naringenin and other excipients are shown in Figure 3.

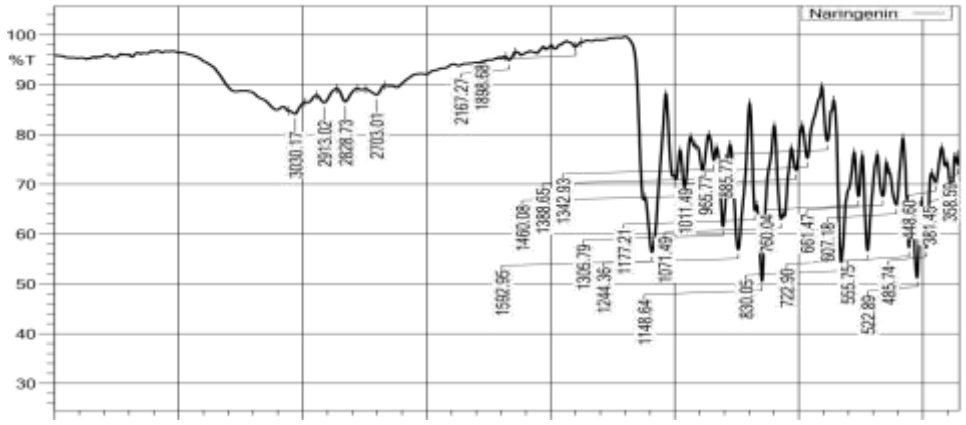

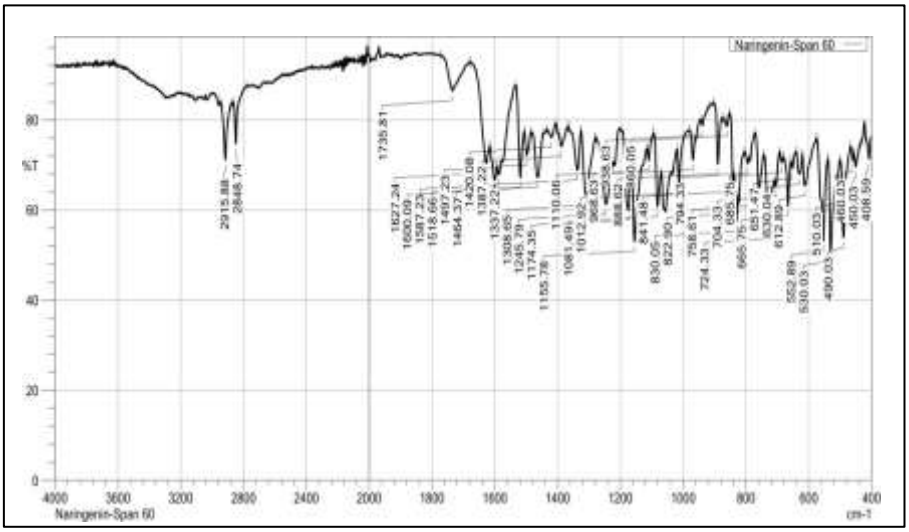

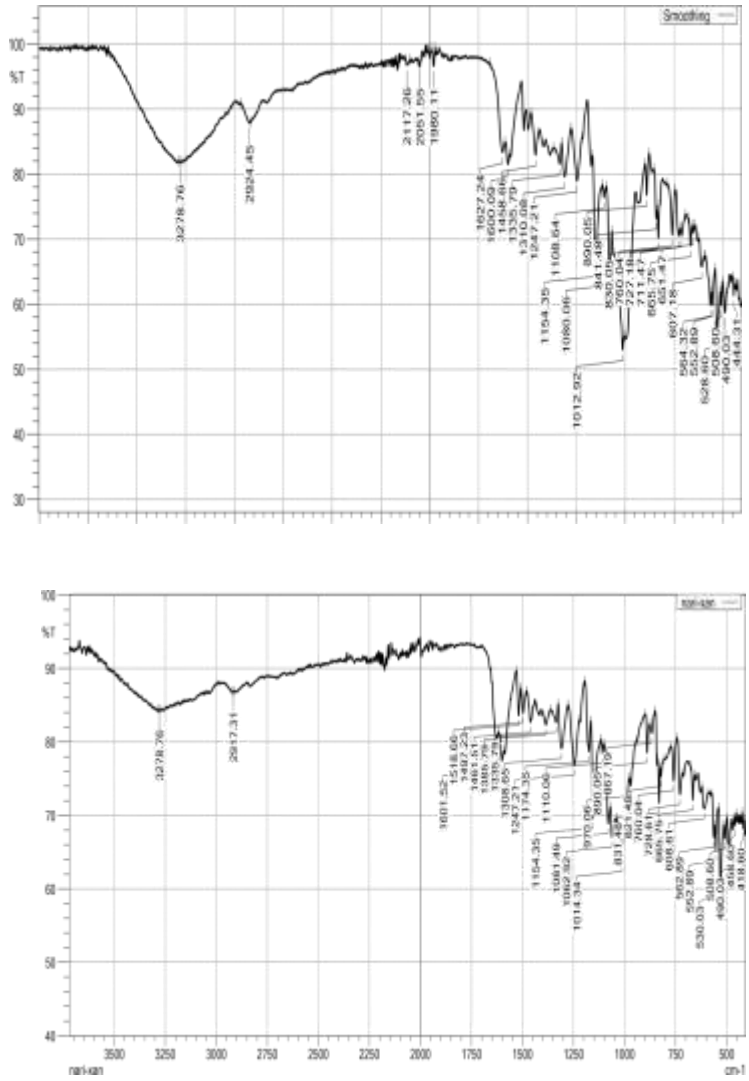

Figure 3: FT-IR Spectra of a). Pure Naringenin, b). Naringenin – Span 60, c). Naringenin – HPMC, d). Naringenin – Xanthum gum

Table no 4: Data obtained from FT-IR Spectral Peaks

Functional Groups	Wave number (cm^{-1}) Literature value	Observed Frequency range (cm^{-1})			
		Pure Naringenin	Naringenin + Span 60	Naringenin + HPMC	Naringenin + Xanthum gum
O–H	3200–3600	3030.17	3030.88	3278.76	3278.76
C–H	3000–3100	2913.02	2915.88	2924.45	2917.31
C=O	1650–1700	1592.95	1755.81	1627.24	1741.35
C=C	1450–1600	1388.65	1600.09	1536.96	1601.52
C–O	1000–1300	1244.36	1246.55	1108.06	1247.45
C–H	650–900	830.05	830.05	830.05	831.48
C–O–C	1000–1300	1011.49	1081.41	1080.06	1154.35

Formulation of Naringenin-loaded Spanlastics

Experimental Design Analysis

Spanlastics were prepared using an ethanol injection method. The concentration of Span 60, Tween 80 and sonication time were found to significantly influence the characteristics of spanlastics, including particle size, zeta potential and %

EE. A 2^3 factorial design was employed to optimize the formulation. Table 5 represents the complete pattern of experimental design along with the actual responses of the trial in the study.

Table 5: The experimental design pattern and the corresponding actual responses of naringenin-loaded spanlastics

Variables				Actual Responses		
Run	**Concentration of Span 60 (X1)**	**Concentration of Tween 80 (X2)**	**Sonication Time (X3)**	**Particle size (Y1)**	**Zeta Potential (Y2)**	**% EE (Y3)**
F1	180	90	4.5	160.2	-35.3	89.4
F2	180	90	9	126.3	-49.2	87.5
F3	180	30	9	185.1	-54.6	75.8
F4	100	90	4.5	158.7	-21	70.6
F5	100	90	9	119.2	-33.4	65.4
F6	180	30	4.5	214.5	-55.8	80.1
F7	100	30	4.5	184.5	-41.4	68.4
F8	100	30	9	142.6	-47.1	54.7

Statistical Analysis for Particle Size

The model F value of 16.9 implies that the model is significant for Particle size (Y_1) and there is 1.07 % chances that a model F value seems to be larger due to the noise for each case. Table 6 outlines the summary of statistical analysis for Y_1 response. From the data obtained, it is observed that the variables X_1 (Concentration of Span 60), X_2 (Concentration of Tween 80) and X_3 (Sonication time) were statistically significant for the response Y_1, as the ($p<0.05$). The quadratic polynomial equation in terms of coded factors is as follows:

Particle size (Y_1) = + 161.39 + 10.14 * X_1 – 20.29 * X_2 - 18.09 * X_3 (1)

According to the polynomial equation, the positive sign of regression coefficient (X_1) signifies the synergistic effect on response variable (Y_1). In other words, as the concentration of Span 60 increases, the particle size also increases, the increased particle size is mainly attributed to the formation of larger vesicular structures due to aggregation and fusion of vesicles. The negative sign of regression coefficient (X_2) signifies antagonistic effect on response variable (Y_1). In other words, as the concentration of Tween 80 increases, the particle size decreases, this can be attributed to its emulsifying and edge-activating properties. Tween 80 reduces the interfacial tension between the aqueous and lipid phases, thereby facilitating the formation of smaller and more stable vesicles. In addition to this, Tween 80 enhances the flexibility and fluidity of the spanlastic membrane, preventing vesicle aggregation and leading to a reduction in particle size. Similarly, the antagonistic effect of (X_3) on response variable (Y_1) is mainly associated with high energy input provided during sonication, which facilitates the breakdown of larger vesicles into smaller ones. The contour and 3D surface plots for particle size are depicted in Figure 4.

Table 6: Summary of statistical analysis for Particle Size

Source	Sum of Squares	DF	Mean Square	F-value	*p-value*
Model	6732.07	3	2244.02	16.09	0.0107
X_1	822.17	1	822.15	5.90	0.0421
X_2	3292.66	1	3292.66	23.61	0.0083
X_3	2617.26	1	2617.26	18.77	0.0123
$R^2 = 0.9235$	Predicted $R^2 = 0.6939$	Adjusted $R^2 = 0.8661$			

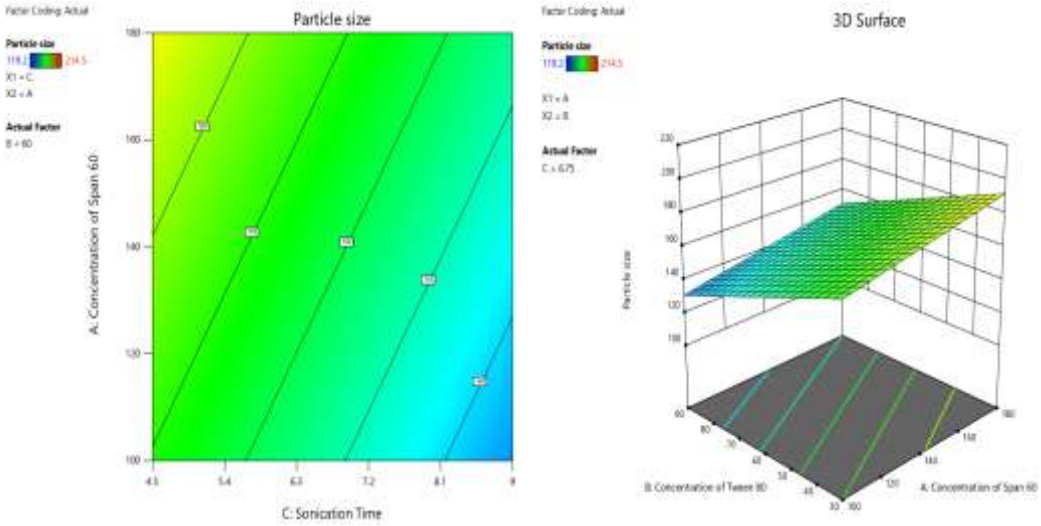

Figure 4: Contour Plots and 3D Surface plots for Particle Size

Statistical Analysis for Zeta Potential

The model F value of 15.06 implies that the model is significant for Zeta Potential (Y_2) and there is 1.21 % chances that a model F value seems to be larger due to the noise for each case. Table 7 outlines the summary of statistical analysis for Y_2 response. From the data obtained, it is observed that the variables X_1 (Concentration of Span 60), X_2 (Concentration of Tween 80) and X_3 (Sonication time) were statistically significant for the response Y_2, as the ($p<0.05$). The quadratic polynomial equation in terms of coded factors is as follows:

Zeta Potential (Y_2) = - 42.23 – 6.50 * X_1 + 7.50 * X_2 – 3.85 * X_3 (2)

According to the polynomial equation, the negative sign of regression coefficient (X_1) signifies the antagonistic effect on response variable (Y_2). In other words, as the concentration of Span 60 increases, the zeta potential decreases, the decreased zeta potential is mainly attributed to the formation of larger and more rigid vesicles at higher surfactant concentration. Furthermore, the non-ionic nature of Span 60 contributes to reduced electrostatic repulsion between vesicles, resulting in a decrease in zeta potential values. The positive sign of regression coefficient (X_2) signifies synergistic effect on response variable (Y_2). In other words, as the concentration of Tween 80 increases, the zeta potential also increases, this can be attributed to enhanced stabilization of vesicles provided by the surfactant. This results in a greater net surface charge around the vesicles, thereby leading to an increase in zeta potential values. Similarly, the antagonistic effect of (X_3) on response variable (Y_2) is mainly associated with an extended sonication, which in-turn disrupts the electrical double layer surrounding the vesicles and reduce the net surface charge, leading to lower zeta potential values. The contour and 3D surface plots for zeta potential are depicted in Figure 5.

Table 7: Summary of statistical analysis for Zeta Potential

Source	Sum of Squares	DF	Mean Square	F-value	*p-value*
Model	906.58	3	302.19	15.06	0.0121
X_1	338.00	1	338.00	16.84	0.0148
X_2	450.00	1	450.00	22.42	0.0091
X_3	118.58	1	118.58	5.91	0.0519
$R^2 = 0.917$	Predicted $R^2 = 0.6746$	Adjusted $R^2 = 0.8576$			

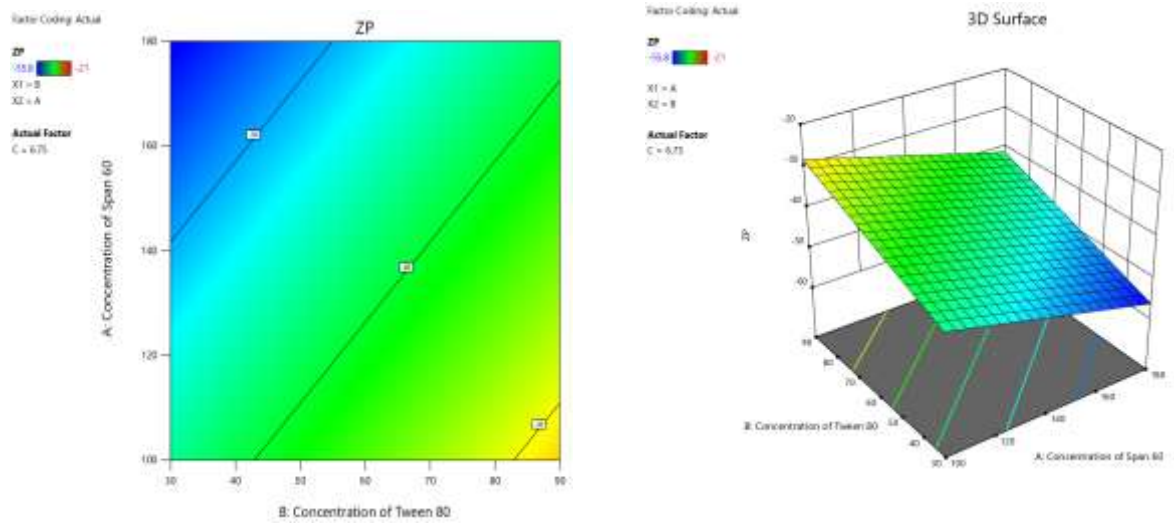

Figure 5: Contour Plots and 3D Surface plots for Zeta Potential

Statistical Analysis for % Entrapment Efficiency (% EE)

The model F value of 25.11 implies that the model is significant for Zeta Potential (Y_2) and there is 0.47 % chances that a model F value seems to be larger due to the noise for each case. Table 8 outlines the summary of statistical analysis for Y_3 response. From the data obtained, it is observed that the variables X_1 (Concentration of Span 60), X_2 (Concentration of Tween 80) and X_3 (Sonication time) were statistically significant for the response Y_3, as the ($p<0.05$). The quadratic polynomial equation in terms of coded factors is as follows:

$$\% \text{ EE } (Y_3) = + 73.99 + 9.21 * X_1 + 4.24 * X_2 - 3.14 * X_3 \quad (3)$$

According to the polynomial equation, the positive sign of regression coefficient (X_1) signifies the synergistic effect on response variable (Y_3). In other words, as the concentration of Span 60 increases, the % EE also increases, the increased % EE is mainly attributed to the enhanced formation of vesicular bilayers, which provide greater space for drug encapsulation. The positive sign of regression coefficient (X_2) signifies synergistic effect on response variable (Y_3). In other words, as the concentration of Tween 80 increases, the % EE also increases, this can be attributed to the edge activator property of Tween 80, improving the fluidity of the vesicular membrane and facilitating better incorporation of the drug within the vesicles. Similarly, the antagonistic effect of (X_3) on response variable (Y_2) is mainly associated with excessive energy generated during prolonged sonication, which can disrupt the vesicular structure and cause leakage of the entrapped drug. The contour and 3D surface plots for % entrapment efficacy are depicted in Figure 6.

Table 8: Summary of statistical analysis for % EE

Source	Sum of Squares	DF	Mean Square	F-value	*p-value*
Model	901.36	3	300.45	25.11	0.0047
X_1	678.96	1	678.96	56.74	0.0017
X_2	143.65	1	143.65	12.00	0.0257
X_3	78.75	1	78.75	6.58	0.0523
$R^2 = 0.9496$	Predicted $R^2 = 0.7983$	Adjusted $R^2 = 0.9118$			

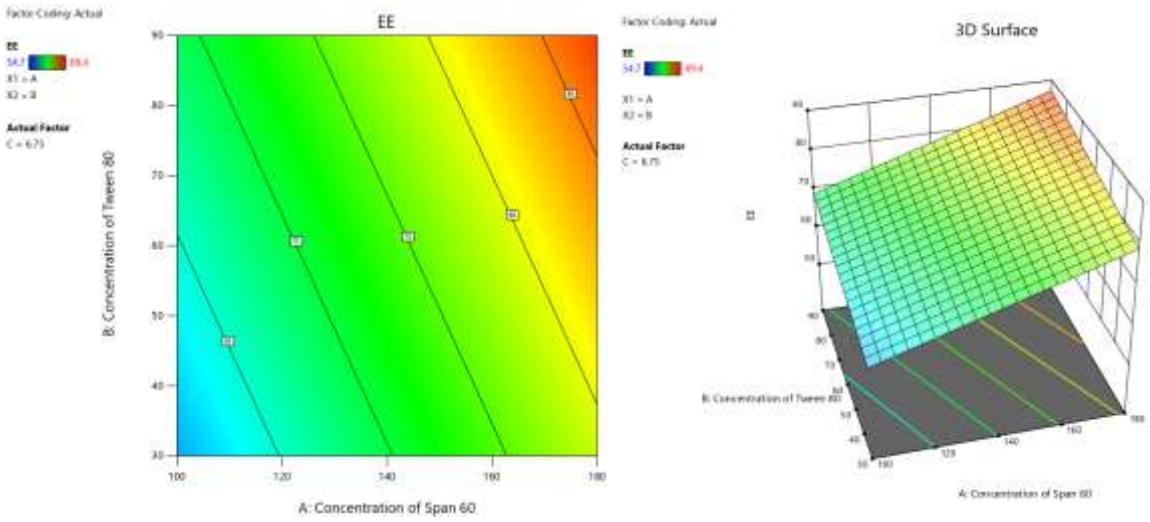

Figure 6: Contour Plots and 3D Surface plots for % Entrapment Efficacy

Optimization of Naringenin-loaded Spanlastic Formulation

The naringenin-loaded spanlastics formulation was optimized using design expert software, in consideration with 123.38 g of Span 60, 73.36 g of Tween 80 and 6.8 min of Sonication time. The optimized formulation was further characterized for particle size, zeta potential and % entrapment efficacy. The overlay plot for optimized Spanlastic formulation is depicted in Figure 7.

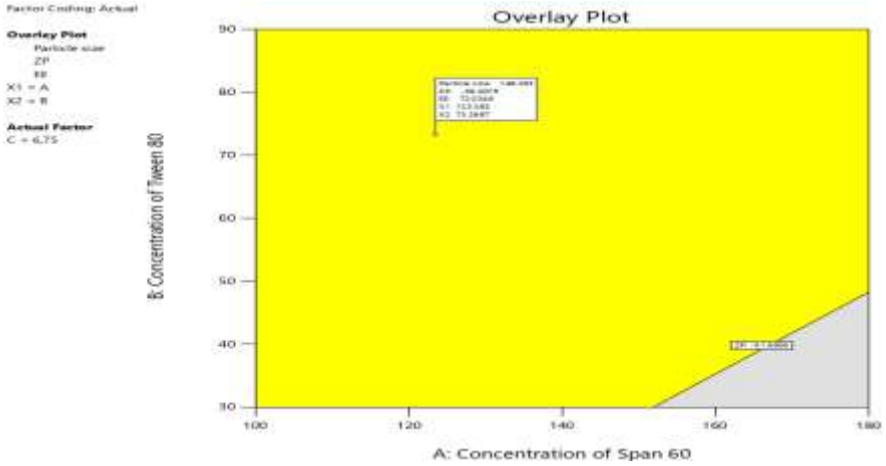

Figure 7: Overlay Plot for Optimized Naringenin-loaded Spanlastic Gel

Particle size and Zeta Potential analysis of Optimized Naringenin-loaded Spanlastics Formulation

The optimized batch exhibited a particle size of 157.7 nm, confirming the nanoscale dimensions of the vesicles. The zeta potential was measured at –32.4 mV, indicating a strong negative surface charge that enhances formulation stability by minimizing particle aggregation. The % EE of optimized spanlastics was found to be 82.95 %. The particle size distribution and zeta potential data for the optimized spanlastics are illustrated in Figure 8. The data obtained for the optimized formulation is shown in Table 9.

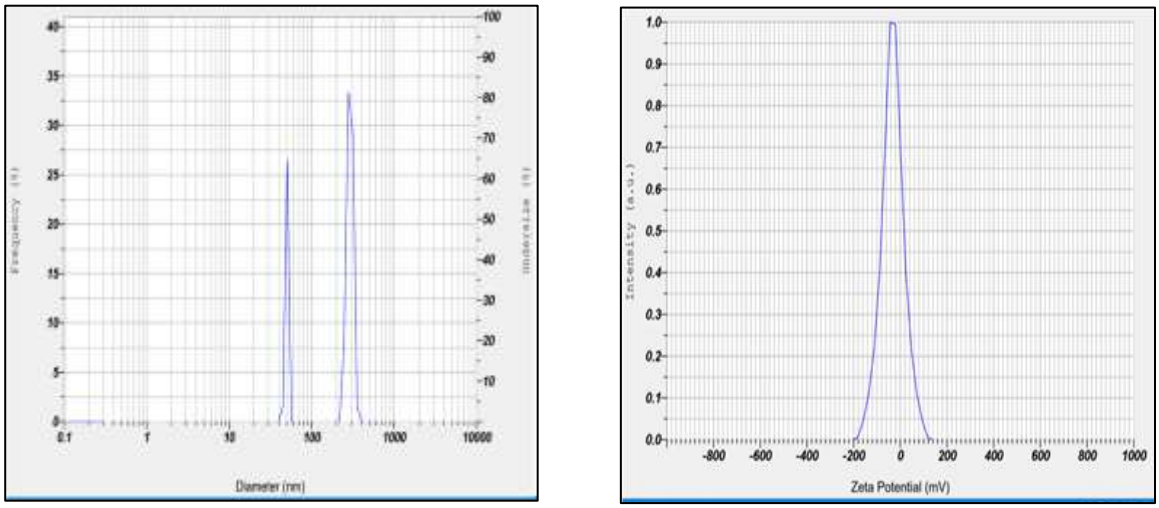

Figure 8: a). Particle size and b). Zeta Potential of Optimized Naringenin-loaded Spanlastic Formulation

Table 9: Optimized formulation of Naringenin-loaded Spanlastics Formulation

S No	Formulation Code	Particle size (nm)	Zeta Potential (mV)	% EE
1	OF1	157.7 nm	-32.4 mv	82.95 %

Drug Content of Naringenin-loaded Spanlastics Formulation

One of the critical parameters for any dosage form is its drug content. The drug content of the optimized Naringenin-loaded spanlastics was around 79.03±1.93%, closely aligned with the entrapment efficiency of the optimized batch.

Morphological Studies

Transmission Electron Microscope (TEM) of Optimized Naringenin-loaded Spanlastics Formulation

TEM analysis of the Spanlastics revealed that, the particles were spherical in shape, and in the nano size range, well isolated from each other. The homogeneous size distribution indicated the stability of the prepared spanlastics. The TEM image of spanlastics are depicted in Figure 9.

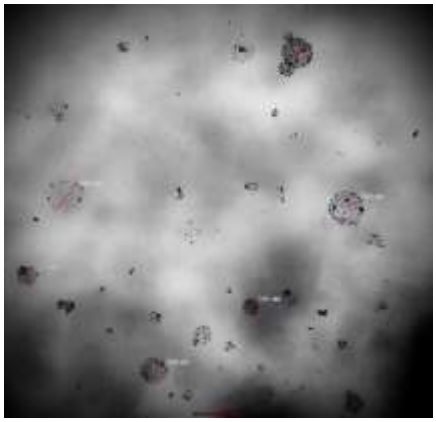

Figure 9: TEM image of Optimized Naringenin-loaded Spanlastic Formulation

Characterization of Naringenin-loaded Spanlastics Topical Gel

Appearance

The color, homogeneity and consistency of the prepared formulations were visually inspected. The topical formulations were pale yellow in color with good homogeneity and consistency.

Determination of pH

A digital pH meter was used to measure the pH of the gel. The pH of the gel formulations ranged from 6.9 ± 0.41 to 7.3 ± 0.23. This pH range is considered suitable for topical application and is close to physiological pH of the skin, thereby minimizing the risk of skin irritation. The results of pH values of naringenin-loaded spanlastics gel are tabulated in Table 10.

Viscosity

The naringenin-loaded spanlastics topical gel exhibited a viscosity in the range of 2884.57 ± 0.65 to 5987.28 ± 0.84 cps, suggesting an optimal consistency for prolonged retention on the skin's surface. This suitable viscosity enables the spanlastics to adhere effectively, ensuring sustained release and enhanced efficacy. Additionally, the naringenin-loaded

spanlastics topical gels rheological properties support its potential for topical applications. The data obtained for viscosity values are shown in Table 10.

Spreadability

Spreadability is an important characteristic of topical gels designed for acne management, as it ensures even distribution over the affected skin. The values of spreadability were found to be 6.8 ± 0.5 to 7.6 ± 0.43 cm. The naringenin-loaded spanlactics topical gel formulation GG3 demonstrated a spread diameter of 7.6 ± 0.43 cm, suggesting good appropriate consistency and ease of application. The data obtained for spreadability values are tabulated in Table 10.

Drug Content

The % drug content of naringenin-loaded spanlastics gel were found to be in the range of 78.22 ± 0.57 to 85.38 ± 0.69 %. The values of drug content analysis of gel formulations are tabulated in Table 10.

Table 10: Evaluation of Naringenin-loaded Spanlastics Gel Formulation

Formulation code	pH	Viscosity (cps)	Spreadability (cm)	% Drug content
GG1	7.1 ± 0.17	2884.57 ± 0.65	6.8 ± 0.52	82.24 ± 0.46
GG2	7.3 ± 0.23	4985.65 ± 0.74	7.0 ± 0.85	80.55 ± 0.25
GG3	6.9 ± 0.41	3562.17 ± 0.47	7.6 ± 0.43	85.38 ± 0.69
GG4	7.2 ± 0.53	5987.28 ± 0.84	6.9 ± 0.23	78.22 ± 0.57

All data are given in mean ± SD, n=3; n is the number of observations

In Vitro Diffusion Study

Naringenin-loaded Spanlastics serve as valuable tool in in-vitro drug diffusion studies. By encapsulating drugs and controlling their release, they offer a platform to optimize drug delivery systems for improved therapeutic efficacy. The in-vitro drug diffusion at 8 hours is influenced by the viscosity and polymer type used in each gel formulation. GG1, containing 1% HPMC and having the lowest viscosity of 2884.57 cps, is expected to show the fastest drug release of 95.366% due to reduced resistance to drug diffusion. GG2, with a higher concentration of HPMC 1.5% and increased viscosity of 4985.65 cps, likely provides a slightly slower release of 89.838% than GG1. GG3, formulated with 1% xanthan gum and moderate viscosity of 3562.17 cps, is expected to release the drug at a more controlled rate of 82.493% because xanthan gum forms a stronger gel matrix that hinders diffusion more effectively than HPMC. GG4, containing 1.5% xanthan gum and the highest viscosity of 5987.28 cps, is anticipated to exhibit the most sustained release 8 hours (71.776%), as the dense gel network significantly restricts drug movement, making it ideal for prolonged topical delivery [19]. The sustained release suggests prolonged residence time and enhanced skin permeation of Naringenin. This behaviour can contribute to reduced dosing frequency and improved patient compliance. Additionally, the nanosize and elasticity of spanlastics aid in deeper skin penetration, making them ideal for topical facial delivery. The graphical representation of in vitro diffusion of naringenin-loaded spanlastics gels are depicted in Figure 10.

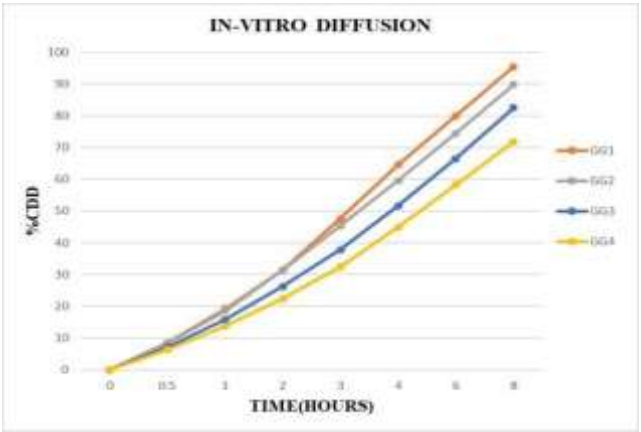

Figure 10: Graphical representation of in vitro diffusion of naringenin-loaded spanlastics gels

Stability Studies

The stability study was conducted at 40 ± 2°C and 75 ± 5% RH for a period of 60 days to evaluate the stability of the developed formulation. The results showed a gradual increase in particle size from 157.7 ± 1.81 nm at day 0 to 172.86 ± 1.78 nm at day 60. This increase may be attributed to slight aggregation or fusion of vesicles during storage. A decrease in entrapment efficiency was observed from 84.69 ± 0.46 % initially to 68.42 ± 1.44 % after 60 days, which could be due to the gradual leakage of the entrapped drug from the vesicular system under accelerated storage conditions. Similarly,

the drug content decreased from 79.03 ± 1.93% to 69.46 ± 2.37 %, indicating a minor loss of drug during storage. The zeta potential values remained negative throughout the study, ranging from −32.4 ± 0.23 mV at day 0 to −29.66 ± 0.66 mV at day 60. Although a slight reduction was observed, the values remained sufficiently high to maintain electrostatic repulsion between vesicles, thereby preventing extensive aggregation and ensuring acceptable colloidal stability. Overall, despite slight changes in particle size, entrapment efficiency, zeta potential, and drug content during storage, the formulation retained its physicochemical characteristics and demonstrated satisfactory stability under accelerated storage conditions for 60 days. Table 11 represents the data obtained for stability studies.

Table 11: Data for short term stability studies

Storage Interval at 40 ± 2°C & 75 ± 5 % RH	Particle Size (nm)	% Entrapment Efficiency	Zeta Potential (mV)	Drug Content (%)
0 Days	157.7 ± 1.81	84.69 ± 0.46	-32.4 ± 0.23	79.03 ± 1.93
30 Days	165.67 ± 0.95	70.88 ± 2.34	-27.8 ± 0.71	71.83 ± 0.98
60 Days	172.86 ± 1.78	68.42 ± 1.44	-29.66 ± 0.66	69.46 ± 2.37

All data are given in mean ± SD, n=3; n is the number of observations

Minimum Inhibitory Concentration (MIC)

The Minimum Inhibitory Concentration (MIC) study was carried out to evaluate the antibacterial efficacy of Naringenin against *Propionibacterium acnes* using serial dilutions ranging from 100 µg/mL to 0.2 µg/mL in thioglycollate broth. The results demonstrated that Naringenin effectively inhibited the growth of P. acnes at concentrations up to 0.8 µg/mL, whereas bacterial growth was observed at 0.4 µg/mL and lower concentrations. Based on these findings, the MIC of Naringenin was determined to be 0.8 µg/mL. The low MIC value obtained in this study indicates the strong antibacterial potential of Naringenin against P. acnes, one of the primary microorganisms implicated in the pathogenesis of acne vulgaris. The ability of Naringenin to inhibit bacterial growth at a relatively low concentration suggests its effectiveness as an antimicrobial agent and highlights its therapeutic potential in acne management. In addition to its antibacterial properties, Naringenin is a naturally occurring flavonoid known for its anti-inflammatory and antioxidant activities, which may further contribute to its beneficial effects in acne treatment. These findings support the incorporation of Naringenin into topical drug delivery systems for the treatment of acne. Its potent antimicrobial activity, coupled with its natural origin and favorable safety profile, makes it a promising bioactive compound for the development of effective and patient-friendly dermatological formulations [20]. Therefore, Naringenin may serve as a valuable therapeutic candidate for controlling *P. acnes*-associated skin infections and reducing acne severity.

DISCUSSION

Acne vulgaris is a widespread, chronic inflammatory skin disorder that primarily affects adolescents, although its prevalence is increasingly noted among adult females. The condition has a complex pathogenesis involving increased sebum secretion, follicular hyperkeratinization, colonization by Cutibacterium acnes, and subsequent inflammation. These pathophysiological factors contribute to various types of acne lesions and can significantly affect patients' quality of life. While several therapeutic options, including topical retinoids, antibiotics, hormonal treatments, and isotretinoin, are currently available, their clinical utility is often restricted due to adverse effects, the emergence of bacterial resistance, and frequent recurrences. These limitations highlight the necessity for more effective and safer alternatives [2].

Naringenin, a naturally occurring flavonoid with notable anti-inflammatory and antioxidant properties, has demonstrated potential in managing acne. However, its poor aqueous solubility and limited permeability through the skin barrier significantly hinder its effectiveness in topical applications. To address these limitations, the present study aimed to enhance the topical delivery of Naringenin through incorporation into spanlastics-elastic nanovesicular carriers composed of nonionic surfactants and edge activators designed to improve dermal penetration, drug stability, and controlled release [8].

Spanlastic vesicles were formulated using the ethanol injection method, employing Span 60 as the primary surfactant due to its bilayer-forming capability and low HLB value, and Tween 80 as an edge activator to enhance vesicle deformability and skin penetration [4]. Pre-formulation studies confirmed the solubility of Naringenin in organic solvents and its compatibility with selected excipients, as evidenced by FTIR and melting point analysis. UV spectrophotometry was used to determine the maximum absorbance wavelength (λmax) for drug quantification in release studies [10].

Optimization of the formulation was conducted using a 2^3 full factorial design. Results indicated that increasing the concentration of Span 60 led to larger vesicle sizes due to bilayer thickening, whereas Tween 80 reduced vesicle size by promoting stabilization of smaller vesicles. Prolonged sonication time contributed to a reduction in vesicle size through vesicle fragmentation. The optimized formulation exhibited favorable characteristics, including a nanoscale particle diameter of 157.7 nm, a high negative zeta potential –32.4 mV, and substantial entrapment efficiency of 89.4%, indicating both physical stability and efficient drug loading. Transmission Electron Microscopy (TEM) confirmed the formation of spherical, uniformly distributed vesicles [20].

The optimized spanlastic formulation was subsequently incorporated into a xanthan gum- based gel to facilitate topical application. The resulting gel displayed acceptable viscosity, pH, drug content, and rheological behavior suitable for dermal use. Xanthum gum provided bioadhesive properties that likely improved the formulation's retention on the skin

surface. Permeation studies using a Franz diffusion cell demonstrated extended Naringenin release attributed to the nanovesicles small size and elasticity, which facilitated stratum corneum penetration [18].
Accelerated stability testing over three months under standard conditions revealed no significant changes in particle size, zeta potential, drug content, or viscosity, thereby confirming the formulation's physical and chemical stability. Furthermore, antimicrobial activity testing indicated that Naringenin retained its effectiveness against acne-causing bacteria, thereby supporting its therapeutic potential [17]. Overall, the developed Naringenin-loaded spanlastic gel offers a promising strategy for the topical treatment of acne vulgaris, overcoming the limitations of conventional therapies through enhanced drug penetration, stability, sustained release, and antibacterial activity.

CONCLUSION

The present study successfully developed and optimized a Naringenin-loaded spanlastics gel for the topical treatment of acne vulgaris. The optimized naringenin-loaded spanlastics formulation exhibited nanosized vesicles, high entrapment efficiency, and good physical stability, enhancing the solubility and skin delivery of Naringenin. Incorporation of the spanlastic dispersion into a xanthan gum-based gel resulted in a formulation with suitable pH, viscosity, and drug content for topical application. The developed gel demonstrated sustained drug release, effective skin permeation, satisfactory stability under accelerated storage conditions, and significant antimicrobial activity against acne-causing bacteria. Overall, the Naringenin-loaded spanlastics gel represents a promising topical delivery system for acne management, offering improved drug delivery, prolonged therapeutic action, and enhanced patient compliance.

Funding
Not applicable

Acknowledgments
Authors would like to extend sincere gratitude for the support provided by KLE Academy of Higher Education and Research (KAHER) for financial assistance and support throughout the research work.

Conflicts Of Interest
The authors declare no conflict of interest

REFERENCES

1. Vasam M, Korutla S, Bohora RA. Acne vulgaris: A review of the pathophysiology, treatment, and recent nanotechnology based advances. Biochem Biophys Rep. 2023; 36:101578.
2. Ansong JA, Asante E, Johnson R, Boakye-Gyasi ME, Kuntworbe N, Akuffo Owusu FW, Ofori-Kwakye K. Formulation and Evaluation of Herbal-Based Antiacne Gel Preparations. BioMed Res Int. 2023; 1: 7838299.
3. Shamma RN, Sayed S, Sabry NA, El-Samanoudy SI. Enhanced skin targeting of retinoic acid spanlastics: in vitro characterization and clinical evaluation in acne patients. J Liposome Res. 2019; 29(3): 283-90.
4. Lakshmi Priya NS, Nanjappa SH, Narhari KV, Nandakumar A, Sharath TP and Yashwanth S. Unleashing the Potential of Spanlastics as Drug Delivery Carrier. J Adv Med Pharm Sci. 2025; 27(5): 33-52.
5. Nadim N, Khan AA, Khan S, Parveen R, Ali J. A narrative review on potential applications of spanlastics for nose-to-brain delivery of therapeutically active agents. Adv Colloid Interface Sci. 2025; 335: 103341.
6. Ansari MD, Khan I, Solanki P, Pandit J, Jahan RN, Aqil M and Sultana Y. Fabrication and optimization of raloxifene loaded spanlastics vesicle for transdermal delivery. J Drug Deliv Sci Technol. 2022; 68: 103102.
7. Rukari T, Pingale P and Upasani C. Vesicular drug delivery systems for the fungal infections treatment through topical application-a systemic review. J Cur Sci Technol. 2023; 13(2): 501-17.
8. Niedźwiedzka A, Micallef MP, Biazzo M, Podrini C. The Role of the Skin Microbiome in Acne: Challenges and Future Therapeutic Opportunities. Int J Mol Sci. 2024; 25(21):11422.
9. Bhia M et.al. Naringenin nano-delivery systems and their therapeutic applications. Pharmaceutics. 2021; 13(2):291.
10. Sumathi R, Tamizharasi S, Sivakumar T. Formulation and evaluation of polymeric nanosuspension of naringenin. Int J App Pharm. 2017; 9(6):60-70.
11. Solanki R, Patel K, Patel S. Bovine serum albumin nanoparticles for the efficient delivery of berberine: Preparation, characterization and in vitro biological studies. Colloids Surf A: Physicochem Eng Asp. 2021; 608:125501.
12. El Hosary R, Teaima MH, El-Nabarawi M, Yousry Y, Eltahan M, Bakr A, Aboelela H, Abdelmonem R, Nassif RM. Topical delivery of extracted curcumin as curcumin loaded spanlastics anti-aging gel: Optimization using experimental design and ex- vivo evaluation. Saudi Pharm J. 2024; 32(1):101912.
13. Sagare RD, Dasankoppa FS, Sholapur HN, Design, optimization and characterization of γ-methacryloxypropyltrimethoxysilane-doped halloysite clay nanotubes using ultra-turrax homogenizer. J Pharm Innov. 2023; 18(2): 719-34.
14. Mousa IA, Hammady TM, Gad S, Zaitone SA, El-Sherbiny M, Sayed OM. Formulation and Characterization of Metformin-Loaded Ethosomes for Topical Application to Experimentally Induced Skin Cancer in Mice. Pharmaceuticals. 2022; 15(6): 657.
15. Aboud HM, Hassan AH, Ali AA, Abdel-Razik ARH. Novel in situ gelling vaginal sponges of sildenafil citrate-based cubosomes for uterine targeting. Drug Deliv. 2018; 25(1):1328–39.
16. Pathan IB, Munde SJ, Shelke S, Ambekar W, Mallikarjuna Setty C. Curcumin loaded fish scale collagen-HPMC nanogel for wound healing application: Ex-vivo and In-vivo evaluation. Int J Polym Mater Polym Biomater. 2019; 68(4):165-74.

17. Patel P, Patel P. Formulation and evaluation of clindamycin HCL in situ gel for vaginal application. Int J Pharm Inv. 2015; 5(1): 50.
18. Alkilani AZ, Alkhaldi R, Basheer HA, Amro BI and Alhusban MA. Fabrication of Thymoquinone and Ascorbic Acid-Loaded Spanlastics Gel for Hyperpigmentation: In Vitro Release, Cytotoxicity, and Skin Permeation Studies. Pharmaceutics. 2025; 17(48):1-23.
19. Antimicrobial susceptibility testing protocols. Schwalve, Moore and Goodwin, Crc Press 2007.
20. Aziz DE, Abdelbary AA, Elassasy AI. Implementing Central Composite Design for Developing Transdermal Diacerein-Loaded Niosomes: Ex vivo Permeation and In vivo Deposition. Curr Drug Deliv. 2018; 15(9): 1330-42.